

The repetitive local sampling and the local distribution theory

Pu Tian^{*,†,‡}

[†]*School of Life Sciences, Jilin University, Changchun, China 130012*

[‡]*School of Artificial Intelligence, Jilin University, Changchun, China 130012*

E-mail: tianpu@jlu.edu.cn

Phone: +86 (0)431 85155287

Abstract

1
2 Molecular simulation is a mature and versatile tool set widely utilized in many subjects
3 with more than 30,000 publications each year. However, its methodology development has
4 been struggling with a tradeoff between accuracy/resolution and speed, significant improve-
5 ment of both beyond present state of the art is necessary to reliably substitute many expensive
6 and laborious experiments in molecular biology, materials science and nanotechnology. Pre-
7 viously, the ubiquitous issue regarding severe wasting of computational resources in all forms
8 of molecular simulations due to repetitive local sampling was raised, and the local free energy
9 landscape approach was proposed to address it. This approach is derived from a simple idea of
10 first learning local distributions, and followed by dynamic assembly of which to infer global
11 joint distribution of a target molecular system. When compared with conventional explicit
12 solvent molecular dynamics simulations, a simple and approximate implementation of this
13 theory in protein structural refinement harvested acceleration of about six orders of magnitude
14 without loss of accuracy. While this initial test revealed tremendous benefits for addressing
15 repetitive local sampling, there are some implicit assumptions need to be articulated. Here, I
16 present a more thorough discussion of repetitive local sampling; potential options for learning

17 local distributions; a more general formulation with potential extension to simulation of near
18 equilibrium molecular systems; the prospect of developing computation driven molecular sci-
19 ence; the connection to mainstream residue pair distance distribution based protein structure
20 prediction/refinement; and the fundamental difference of utilizing averaging from conventional
21 molecular simulation framework based on potential of mean force. This more general devel-
22 opment is termed the local distribution theory to release the limitation of strict thermodynamic
23 equilibrium in its potential wide application in general soft condensed molecular systems.

24 **Introduction**

25 Molecular simulation has been utilized in a wide variety of disciplines, including but not limited
26 to chemistry, physics, biology and materials science. Its increasing importance is clearly demon-
27 strated by steady growth of relevant publications as shown in Fig. 1. However, atomistic molecu-
28 lar dynamics (MD) simulations, while being effective in revealing underlying atomic mechanisms
29 for many molecular processes, are extremely computationally intensive.^{1,2} Historically, scientists
30 have developed two lines of algorithms to accelerate molecular simulations, with one being coarse
31 graining (CG)³⁻¹² and the other being enhanced sampling (ES).¹³⁻¹⁶ Realizing that there is severe
32 wasting of computational resources due to repetitive local sampling (RLS) in all molecular simu-
33 lations, the local free energy landscape (LFEL) approach was proposed to eliminate such wasting,
34 and its effectiveness was subsequently demonstrated in an approximate implementation in protein
35 structural refinement.¹⁷ The connection among CG, ES and LFEL as various forms of applying “di-
36 viding and conquering” and “caching” principle in molecular modeling was summarized.¹⁸ In our
37 initial testing of this new theory, LFEL for amino acid packing in proteins was constructed based
38 on a simple neural network implementation of generalized solvation free energy (GSFE) theory.¹⁹
39 Further, a computational graph was established through combination of automatic differentiation,
40 coordinate transformation and LFEL cached in trained neural networks. This computational graph
41 was successfully utilized to achieve the only end-to-end and the most efficient protein structural re-
42 finement pipeline¹⁷ up to date. Like all present protein structure prediction, design and refinement

43 studies,^{20–29} there is an implicit and extremely crude assumption that all high resolution experimen-
44 tal structures were solved under similar environmental (thermodynamic) conditions. Alternatively,
45 differences in thermodynamic and environmental conditions are deemed not important for all high
46 resolution structural data utilized to train models. Such assumptions are apparently not true. Addi-
47 tionally, the LFEL approach as it stands only applies to equilibrium conditions. Here, I explicitly
48 articulate these issues, develop a more general form of the LFEL idea and termed it the local distri-
49 bution theory (LDT). Meanwhile, more concrete discussions of RLS, more options for fitting local
50 distributions, extension of LDT to near-equilibrium scenarios, connection of LDT to present AI-
51 based protein structural studies, and the difference of LDT from conventional molecular simulation
52 framework based on potential of mean force are presented. It is hoped that this work will intrigue
53 more interest in further development of LDT in general chemical and biomolecular systems, and
54 facilitate advancement of computation driven molecular science.

55 **Repetitive local sampling**

56 In molecular simulations, we have a long history of utilizing RLS in analysis of MD trajecto-
57 ries. For example, when computing pair distribution function $g(r)$ between oxygen atoms of water
58 molecules, instead of counting a specific pair of water molecules or water molecules within a
59 given small space and binning distances of oxygen atom pairs, statistics is usually accumulated by
60 counting all pairs of water molecules within half simulation box distance to obtain a more smooth
61 curve. Similar tricks are routinely utilized in various analyses of molecular simulation trajectories.
62 The basis of these manipulations is the belief that all molecules of the same chemical identity and
63 composition are indistinguishable, and ensemble average converges to time average for ergodic
64 systems. From a different perspective, all above practice clearly demonstrates that we have been
65 carrying out RLS in essentially all our simulations, except not carefully thinking about its potential
66 utility in saving computational resources in the simulation/sampling stage. This issue was raised
67 previously^{17,18} without sufficiently detailed discussions. Some typical examples of RLS in various

68 simulation and/or modeling applications are discussed below.

69 RLS consumes overwhelming majority of computational resources in regular molecular sim-
70 ulations and exist both within a single simulation task and across different ones. As shown in
71 Fig. 2a, there is a simulation of aqueous solution comprising a few different types of ions and
72 water molecules, with gas-liquid and liquid-solid interfaces under given thermodynamic condi-
73 tions. After a sufficiently long simulation run, if all snapshots were utilized to analyze distribution
74 of molecules and ions in a bulk spherical space A , one would have obtained a converged LFEL,
75 which is a complex high dimensional distribution that gives correct statistical weight for each
76 thermally reachable structural ensemble (or free energy local minimum) on the one hand, and all
77 possible transition paths connecting these minima with respective statistical significance on the
78 other hand. The exactly same LFEL would have been obtained if another bulk spherical space B
79 with the same volume was taken. As a matter of fact, the exactly same LFEL would be obtained
80 for all possible bulk spherical spaces with the same volume. However, for each such separate local
81 space, significant computational resource was consumed to obtain the exactly same result! This is
82 a typical case of RLS in the same simulation task.

83 While local spaces near various interface certainly have LFELs different from that of bulk,
84 there are regularities that can be learned as well. Such RLS may be effectively described from
85 a slightly different perspective according to the GSFE theory as shown in Fig. 2b. In GSFE
86 theory, each comprising unit of a molecular system is on the one hand a solute unit solvated by
87 its surrounding units, and on the other hand a comprising solvent unit for each of its surrounding
88 units. As all units with the same chemical identity/structure are indistinguishable, so should be
89 LFEL of their local solvent under given thermodynamic conditions if a simulation trajectory is
90 sufficiently long. When our focus is on LFEL surrounding a central unit, different scenarios of
91 interfaces are simply different solvent configurations with corresponding statistical weights and
92 no special treatment is required. More specifically, for a water molecule absorbed on wall of a
93 tube filled with water, its solvent units include both water molecules and molecules belong to
94 the wall surrounding it. To eliminate difficulty of defining interfaces at molecular scales is the

95 very initial motivation for development of the GSFE theory. Additionally, defining local spaces
96 with local coordinates originated from individual molecule is a convenient, efficient and natural
97 choice with two advantages. Firstly, it reduces data requirement and improves accuracy during
98 training/learning of local distributions, and secondly, it facilitates assembly by eliminating the
99 uncertainty of selecting from infinite possible origins for local spaces during inference for global
100 joint distribution (GJD) of a target molecular system.

101 Beyond the illustration in Fig. 2, there are other less obvious forms of RLS. For example,
102 in protein structure prediction, design and refinement with implicit representation of aqueous so-
103 lution, each residue in a chain has more or less unique surroundings and no direct RLS seems
104 existing. However, in these tasks, each residue experiences many rounds of adjustment or repack-
105 ing, sampled collisions, favorable and unfavorable configurations from each round is partially or
106 completely discarded and performed on the fly in the next round, engendering significant RLS.
107 Much more computational resource are consumed by RLS across different tasks. Imagine how
108 many times simulations of local packing for water molecules of each popular water force fields
109 have been carried out by thousands of scientists globally! Similarly, packing of amino acids sur-
110 rounding each of 20 natural amino acids have been carried out numerous times by computational
111 structural bioinformaticians around the world. Such RLS is apparently ubiquitous for simulations
112 of all molecular systems.

113 Sufficient sampling of complex molecular system has long been our pursuit in our simulation
114 studies. The very fact that we almost always collect statistics from different local spaces and/or
115 utilize indistinguishable property of molecules for better statistics indicates that we rarely achieve
116 sufficient sampling for a given small space or surrounding of a given single molecule. Therefore,
117 it is likely that more accurate global correlations would have been obtained if sufficient statistics
118 was available for all local regions. Since construction of global distributions by assembly of LFEL
119 realizes this very condition, the ability to cache and utilize LFEL properly would not only tremen-
120 dously reduce amount of computational resources, but also potentially improve accuracy due to
121 effectively more sufficient “local sampling”. This is in strong contrast to decades of trade-off in

122 molecular simulation that improved efficiency being always accompanied more or less by reduced
123 accuracy, and increased efficiency being always accompanied by more or less reduction of ac-
124 curacy! When compared with conventional molecular mechanical force fields^{30–33} or knowledge
125 based potentials,^{34–36} the ability of accounting for many-body correlations is another advantage of
126 LFEL that is likely to contribute to improved accuracy. It is important to note that many neural
127 network based force fields (NNFF) methodologies have been developed up to date.^{37,38} Essentially,
128 development of NNFF and other machine learning based force fields is the mainstream of research
129 bridging artificial intelligence (AI) and molecular simulations with many great successes. NNFF
130 tackles many body correlations and demonstrates improved accuracy while sacrifice some effi-
131 ciency, and remains in the established framework of “force fields + sampling” without considering
132 RLS.

133 **The local distribution theory**

It is well understood that the folding process and conformational distributions for a given protein depend upon both its sequence and environmental conditions. However, due to lack to data, in both establishment of traditional knowledge based potentials^{34–36} and deep learning studies^{21,22} of protein folding, design and structural refinement, it is widely assumed that all experimental structural data may be deemed as obtained under similar conditions, and details of which may be safely ignored in such tasks. Such simplification was similarly utilized in implementing the LFEL approach in protein structure refinement¹⁷ with focus being on coordinates without attending to thermodynamic and solvent conditions. Should detailed modeling of the variation of interested molecular systems under different environmental and/or thermodynamic conditions is desired, inclusion of these variables was essential. Here, previous simplified formulation is extended to deal with such scenarios. Denote environmental and thermodynamic variables (e.g. temperature, pressure, concentrations of relevant molecular species, special restraints) as $\Phi = (\phi_1, \phi_2, \dots, \phi_k)$, molecular coordinates as $X = (x_1, x_2, \dots, x_n)$ and local regions of molecular

systems as $R = (R_1, R_2, \dots, R_m)$ ($m \leq n, m = n$ is preferred), the global joint probability density may be expressed by local distributions $P(\Phi, R_i)$ and their correlations as:

$$\begin{aligned}
 P(\Phi, X) &= P(\Phi, R) \\
 &= \frac{P(\Phi, R)}{\prod_{i=1}^m P(\Phi, R_i)} \prod_{i=1}^m P(\Phi, R_i)
 \end{aligned} \tag{1}$$

134 It is important to note that each R_i ($i = 1, 2, \dots, m$) represents a dynamic collection of molecular
 135 coordinates for the i th specified region and its composing units may change with propagating tra-
 136 jectories. When ($m = n$) or m is close to n , since each local region contains dozens of or more
 137 particles, overlapping among such regions are extensive. Local distributions are essentially LFEL
 138 for equilibrium systems. The fraction term $\frac{P(\Phi, R)}{\prod_{i=1}^m P(\Phi, R_i)}$ includes all complex global correlations
 139 among various local regions R_i ($i = 1, 2, \dots, m$) and is denoted the global correlation factor (GCF)
 140 previously.¹⁸ The product term (hereafter “local term”) $\prod_{i=1}^m P(\Phi, R_i)$ is simply to treat all local re-
 141 gions as if they were independent. If the GCF was ignored, then overlapping parts of different R_i
 142 may have distinct states. In reality, regardless of how many different local regions a molecule x_i
 143 participates, it has a unique physical state at any given instant. So all possible configurations with
 144 contradicting molecular states for any molecule participating different local regions have probab-
 145 ility density zero. Such correction and additional modification of probability density is achieved by
 146 the GCF term. However, direct calculation of GCF is intractable for any realistic complex molec-
 147 ular system. Therefore, equation 1 is not directly useful for understanding and predicting behavior
 148 of molecular systems. How to approximately and effectively utilize this equation in practice is an
 149 open problem, and likely with many potential approximate solutions.

150 Probability density (free energy in equilibrium) of a specific configuration may be decomposed
 151 into three approximately independent contributions. The first is the short range contribution (F_{SR})
 152 that measures the extent of structural stability/compatibility within each local region and is quanti-
 153 fied by the local term in equation 1. The second contribution is from mediated interactions (F_{MED}
 154 Fig. 3ab) that measures the extent of compatibility among all overlapping local regions, and the

155 third contribution measures direct long range (F_{LR} , Fig. 3b) compatibility within the whole molec-
 156 ular system. Both the second and the third contributions are contained in the GCF term. With the
 157 assumption that mediated interactions are independent from long-range interactions, the GCF may
 158 be approximately split into F_{MED} and F_{LR} as shown below.

$$159 \quad \frac{P(\Phi, R)}{\prod_{i=1}^m P(\Phi, R_i)} \approx \exp(-\sum F_{MED}(\Phi, R)) \exp(-\sum F_{LR}(\Phi, R)) \quad (2)$$

160 The summation is over all mediated and long-range interactions in the given configuration R . In
 161 practical computation, separation of F_{SR} and F_{MED} is challenging on the one hand and inefficient
 162 on the other hand. In the previous implementation F_{SR} and F_{MED} were merged. Specifically, As
 163 shown in Fig 3b, at any given instant, a molecule (particle) in the system experiences free energy
 164 driving force additively from local distributions centered on each of its directly interacting neigh-
 165 bors within a preset cutoff. This is in strong contrast to regular MD simulations in which a particle
 166 experience direct forces from its directly interacting neighbors. While F_{LR} was not accounted for
 167 previously, it may be added in for each particle in each or every few propagation step(s). So in
 168 equation 1, local interactions are separated from the GCF, which may be approximately decom-
 169 posed into mediated and long range interactions. However, local and mediated interactions were
 170 computed together in the previous implementation. This choice is somewhat counter intuitive but
 171 is feasible and efficient. Since an analytically clean mathematical factorization of the GCF is not
 172 available, it is likely that the above approximation is just one of many possible ways to realize
 173 practical computation. Distinct molecular systems may have different correlation characteristics
 174 and the optimal approximation is likely to be system specific. Nonetheless, the overall idea is quite
 175 clear, that is to first train local distributions, which are subsequently to be assembled to compose
 176 the GJD according to suitable approximation of the equation 1. The core idea of the LDT is to use
 177 local distributions to eliminate RLS.

178 In a proper implementation of LDT, a target molecular system may be propagated similarly as
 179 in the case of MD simulations except for the two differences. The first difference is that empirical

180 potentials driving MD is replaced by approximate GJD assembled from LDTs. The second is that
181 a learning rate α_a , which is implicitly related to temperature, needs to be given. It is important to
182 note that LDTs are utilized to replace RLS, not global sampling. To accelerate global sampling of
183 a given molecular system, the propagation may be carried out in different temperatures other than
184 the one corresponding to the training data. Methodologies such as simulated annealing³⁹ may be
185 realized just as in regular MD or MC simulations simply by assign a proper scheme of temperature
186 cycles specified by corresponding gaussian noise term with variance α_b . In practice, α_a and α_b
187 need not be identical in the following Langevin equation:

$$188 \quad X_{t+1} = X_t - \alpha_a \frac{\partial(\sum F_{SR} + \sum F_{MED} + \sum F_{LR})}{\partial X} + \epsilon, \epsilon \sim \mathcal{N}(0, \alpha_b) \quad (3)$$

189 **Challenges and options for fitting local distributions**

190 Training/learning of local terms is by no means trivial. In reality, strictly normalized local distribu-
191 tions is beyond reach and we may approximate them by complex high dimensional unnormalized
192 potential functions. The direct consequence of lacking normalization is that resulting free energy
193 unit is arbitrary and is different for different molecular systems. When direct long range interac-
194 tions are to be added, or comparison of results among different molecular systems are essential,
195 this uncertainty has to be resolved. If long-range interactions with fixed unit may be calculated
196 accurately, then it can serve as a unit-defining quantity among different molecular systems.

Construction of local distributions is essentially a density estimation problem in high dimen-
sional space. Firstly, each local region need to be represented mathematically in a translation, rota-
tion and permutation invariant way for its probability density to be effectively fit. Such processing
of molecular coordinates is accomplished by descriptor functions, which have accompanied devel-
opment of neural network force fields (NNFF),^{38,40} and are quite well understood. One possible
way of defining a local region is to utilize the position of an given particle as origin for the local
coordinates, so $R_i = (x_{i-c}, y_{i-s})$, with x_{i-c} being the origin of the local coordinates defined by a

given unit and y_{i-s} being the coordinates of all surrounding molecules within a preset cutoff. It is important to note that the number of molecules may fluctuate and so is dimensionality of y_{i-s} , and padding is a feasible way to address it. The distribution of a local region within a molecular system under environmental conditions Φ may be decomposed into local prior $P(\Phi, y_{i-s})$ and local likelihood $P(\Phi, x_{i-c}|\Phi, y_{i-s})$ as shown below:

$$\begin{aligned} P(\Phi, R_i) &= P(\Phi, x_{i-c}, y_{i-s}) \\ &= P(\Phi, x_{i-c}|\Phi, y_{i-s})P(\Phi, y_{i-s}) \end{aligned} \quad (4)$$

197 The likelihood term measures extent of match between the particle at the origin (x_{i-c}) and its
198 surroundings. The prior term represent structural stability of the surrounding under given environ-
199 mental conditions. In the protein structure refinement implementation,¹⁷ identities of the central
200 amino acids were utilized as labels to train a simple neural network representing likelihood terms,
201 and prior terms were approximated with simple weights. This strategy is likely to be not very
202 useful for general molecular systems. For example, in a typical molecular system of dilute aque-
203 ous solution, the fraction of water molecules is the overwhelming majority. Training with identity
204 will face extremely unbalanced data and important differences among minority molecular/ionic
205 species are likely to be lost. To improve fitting of local distributions, accurate description of both
206 likelihood and prior terms are essential.

207 Like any density estimation application, fitting of local distributions may be carried out di-
208 rectly without decomposing into likelihood and prior terms. As a matter of fact, density estimation
209 problem is of fundamental importance in both statistics and machine learning. Not surprisingly,
210 many neural network architectures have been developed to tackle density estimation in high di-
211 mensional space where conventional methods (e.g. kernel density estimators⁴¹) are not effective.
212 The most widely utilized two types are autoregressive models⁴² and normalizing flows.^{43,44} The
213 former decompose a target joint density into product of conditional densities, which are modeled
214 by parametric densities (e.g. mixture of gaussians) with trainable parameters. The later utilizing

215 invertible neural network architectures to realize a direct quantitative map from a known density
216 (e.g. uniform or gaussian) to the target density space. Establishment of proper correlations among
217 different parametric densities is a highly challenging task for autoregressive models. The invert-
218 ibility requirement in normalizing flow methodology imposes heavy restrictions on neural network
219 architecture and hence its representation power. One outstanding application example of normal-
220 izing flow in modeling molecular system is the Boltzmann generator (BG).⁴⁵ However, application
221 of BG in complex molecular system remain to be tested. The fundamental difference between
222 BG and LDT is that the former aims to directly model GJD for target molecular systems while
223 the later decompose the problem into fitting and assembly of local distributions. Therefore RLS
224 across different tasks is not addressed by BG, which as a results loses transferability of computed
225 results among different molecular systems. A recent more general approach, Roundtrip,⁴⁶ was
226 proposed to overcome weakness of these two density estimation methodology. However, it takes
227 an expensive sampling step to finalize the density estimation. Each available class of methods has
228 its pros and cons, and no theory is available for selection of proper density estimation methodology
229 presently. It might well be that better methods will arise in future. For fitting local distributions
230 in specific complex molecular system, many tests are likely necessary to construct a proper neural
231 network model. Different molecular systems may have distinct structural distributions and case by
232 case exploration is probably necessary to achieve high accuracy.

233 Energy based models (EBM)^{47,48} are good candidates for fitting local distributions, either as a
234 whole or when decomposed into priors and likelihood terms. In EBM, an energy is trained to be as-
235 sociated with a given configuration, thus eliminating the need of a normalization constant, which is
236 a core challenge in fitting local distributions. Present tests of EBMs are mainly in conventional ma-
237 chine learning application scenarios such as computer vision or natural language processing.⁴⁹⁻⁵²
238 Density distributions for such systems are quite different from complex molecular systems of con-
239 densed matter. Since LDT is a new development, significant effort is necessary to search for both
240 proper loss functions, neural network architectures, optimization algorithms and their combina-
241 tions for EBM to facilitate fitting local distributions in our interested molecular systems.

242 While neural networks have been black boxes with exceptional fitting capability up to date, and
243 have been utilized with a wide variety of architectures. Efforts are undergoing for building white
244 box neural networks.⁵³ To realize more physically interpretable and mathematically elegant fitting
245 of local distributions transparently is certainly an attractive potential direction to explore.

246 **Connection to conventional AI driven protein structure studies**

247 Contact map has played a critical role in development of protein structure prediction.²⁹ Earlier
248 contact was a simple binary assignment (contact or not) defined by a cutoff distance based mostly
249 on C_β atoms,²⁹ later on it evolved into residue pair distance distributions (RPDD).^{20,24,25,27} Sig-
250 nificant effort has been invested in investigating impact of various input information and neural
251 network architectures on RPDD prediction with great progress in understanding. As the only
252 known fully end-to-end and the most efficient protein structure refinement and dynamic simula-
253 tion pipeline, GSFE-refinement¹⁷ has a distinct overall pipeline from RPDD based algorithms of
254 protein structure prediction/refinement. With the common goal of describing protein structures,
255 these seemingly very different procedures have to be somehow connected. Fundamentally, all
256 methodologies targeting protein structures reflect their underlying free energy landscape from cer-
257 tain perspective. In GSFE-refinement, the GJD assembled from local distributions (or LFEL) lacks
258 direct long-range correlations beyond spatial range of mediated interactions (Fig. 3) as the method
259 stands now. Certainly, addition of long-range correlations is feasible as already discussed above,
260 and is in fact one important task in our future development plan. Sequence information is limited
261 to the target protein itself in contrast to RPDD based methods, where multiple sequence align-
262 ment (MSA) information is usually included as input. In AlphaFold,²⁰ AlphaFold2⁵⁵ and many
263 other RPDD based studies,^{21,22,24-29,54,56} the core information obtained is explicit protein (family
264) specific RPDD, which are in fact marginalization of the GJD after integrating away all other
265 variables except the distance between the concerning residues. While marginalization in general
266 is an extremely difficulty task in high dimensional space, it is trivial for any known GJD confined

267 within corresponding manifold. Complex neural networks in RPDD based methods essentially re-
268 alize a fitting from input information (protein sequence and MSA) to these marginal distributions
269 without explicit construction of the GJD, approximation of which is the very goal of LDT based
270 methods/models. As shown in Fig. 4, mapping from GJD to RPDD is readily achievable through
271 marginalization. It is important to note that it takes some number of propagation steps (depending
272 upon ruggedness of the underlying FEL) to obtain approximate GJD of sufficient accuracy assum-
273 ing the underlying local distributions are sufficiently accurate. Marginalization is a deterministic
274 procedure with significant loss of information, specifically correlations among different RPDD.
275 Conversely, with RPDD, one may in principle construct GJD with sufficient sampling and opti-
276 mization with necessary restraints. However, since correlations among different RPDD are absent,
277 resulting GJD is highly dependent upon parameters and algorithms utilized in the corresponding
278 reconstruction process. Present mainstream AI-based protein structural prediction/refinement neu-
279 ral networks implicitly cache some projections of local distributions and rules for assembling them
280 into RPDD, each comes with its own loss of information that is hard to retrieve. LDT theory aims
281 to first directly and explicitly learn local distributions, which are subsequently dynamically assem-
282 bled to construct the most comprehensive GJD. LDT thus has the full potential to perform dynamic
283 modeling of relevant molecular processes as long as local distributions were fit for corresponding
284 conditions. However, extending GSEF-refinement for accurately modeling dynamic protein fold-
285 ing is certainly not trivial as data on intermediate states are scarce presently. Nevertheless, LDT
286 is a general theory applicable to any soft condense matter as long as fitting of corresponding local
287 distributions is accomplished.

288 **Potential extension to near equilibrium scenarios**

At molecular scale, temperature, pressure and concentration of comprising molecules have signifi-
cant fluctuations. In conventional MD simulations, temperature and pressure are usually controlled
by various thermostats and barostats⁵⁷ with equilibrium assumption. If we have a heterogeneous

cell being heated at one side, specifying temperature and pressure within it is a challenge. It might well be that both temperature and pressure are heterogeneous in a live cell (sometimes or always) and we just have no proper way of measuring. To specify temperature and pressure with thermostats and barostats is difficult in such scenarios since we have no information on heterogeneous temperature in the first place. The probabilistic description of both molecular coordinates and thermodynamic/environmental variables can be of great utility. Assume the target molecular system is near-equilibrium. More specifically, all local distributions in target molecular system are well approximated by local distributions trained from equilibrium data while global molecular system is off equilibrium (e.g. having temperature/pressure gradient). In such scenario, we need thermodynamic variables to be associated with each local distributions. If the number of local regions was defined as the same as number of molecules/particles, we would have a set of relevant variables associated with each particle $\Phi_i = (\phi_{i1}, \phi_{i2}, \dots, \phi_{ik})$ and denote the environmental conditions as $\Phi = (\Phi_1, \Phi_2, \dots, \Phi_n)$ The equation 1 may be expanded as shown below:

$$P(\Phi, R) = \frac{P(\Phi, R)}{\prod_{i=1}^m P(\Phi_i, R_i)} \prod_{i=1}^m P(\Phi_i, R_i) \quad (5)$$

289 With near-equilibrium assumption, we may safely learn local distributions from data collected in
 290 equilibrium states and relevant environmental conditions. However, propagation of global molec-
 291 ular systems by dynamic assembly of such local distributions is significantly more challenging.
 292 Continuity restraints of relevant Φ variables is probably necessary, this may be realized through
 293 smoothing within certain spatial range. For equilibrium system, propagation of a molecular sys-
 294 tem under thermal fluctuation may be carried out with Langevin equation (equation 3) with a
 295 white noise term associated with a given temperature. However, in near equilibrium scenario, two
 296 choices maybe need to be made for propagating the molecular system. The first is utilize either
 297 maximum likelihood or bayesian approach to determine control variable at each molecule, with
 298 later being significantly more expensive. The second choice is to select a proper smoothing pro-
 299 cedure to prevent large variance in control variables during the inference process. Assuming that

300 local distributions $P(\Phi_i, R_i)$ has been learned with high accuracy, similar assembly and propagation
301 procedures may be utilized as in the equilibrium case except with Φ included and stochastic forces
302 added according to corresponding temperature at each molecule. Large variance of parameters
303 such as temperature and pressure may derail such simple treatment. Significant exploration and
304 development is necessary in these regards. Nonetheless, this opens a potential highly efficient and
305 probabilistic pathway for treatment of near equilibrium massive complex molecular systems (e.g.
306 a cell).

307 **Rapid automatic search for implicit manifold**

308 Due to both local and long range interactions/correlations in condensed molecular systems, the
309 real dimensionality of which is significantly smaller than that corresponds to nominal number of
310 degrees of freedom (DOF). For example, considering 1000 rigid water model molecules in a rigid
311 box, each with 6 DOFs. Its nominal number of DOF for the molecular system is 5997 but its real
312 dimensionality is an unknown but significantly small number dependent upon environmental vari-
313 ables (e.g. temperature, pressure, container material). Local excluded volume interactions, Van
314 der Waals interactions, hydrogen bonding networks, dipolar and multipolar interactions all con-
315 tribute to correlations and dimensionality reduction in water. Conventional way of understanding
316 underlying manifolds for molecular systems is to perform dimensionality reduction analysis on
317 sufficiently sampled trajectories. However, popular principal component analysis (PCA) does not
318 treat nonlinear correlations properly, and many nonlinear algorithms have their own limitations.³⁸
319 More importantly, these dimensionality reduction methodologies are usually utilized as a post pro-
320 cessing step for understanding molecular systems after expensive sampling dominated by RLS has
321 been performed. So the goal is to understand manifolds as one of terminal goals, rather than utiliz-
322 ing manifolds to reduce computational cost. Dynamic assembly of local distributions is, however,
323 fundamentally an implicit manifold search process on the one hand, and utilizes manifolds to re-
324 duce consumption of computational resources on the other hand. Learned local distributions are

325 essentially implicit local manifolds under relevant conditions. Upon assembly of local distribu-
326 tions in propagation driven by derivatives of approximate instantaneous GJD density with respect
327 to coordinates, a molecular system either stay on its manifold (free energy valleys) with fluctua-
328 tions dependent upon temperature or rapidly return to the manifold when being away from it. To
329 state alternatively, construction of GJD by assembly of local distributions according to equation 1
330 is equivalent to construction of global manifold by stitching together local manifolds embedded in
331 local distributions without any manual intervention.

332 It is interesting to note that when viewed from the manifold perspective, LDT is effectively
333 a completely automatic, significantly more accurate and efficient implicit counterpart of Metady-
334 namics when local distributions were fit accurately and assembled properly. In Metadynamics,
335 one first guess or compute for guiding collective variables (CVs), which is essentially an explicit
336 and significantly simplified representation of the manifold for a target molecular system in a given
337 coordinate system. This is a highly challenging task, usually some iterative process is necessary
338 but accuracy of resulting CVs has no guarantee, and no systematic theory is available for explicit
339 searching of CVs. Subsequently explicit biases are accumulated to compute probability density of
340 visited segments along CVs. In a properly implemented LDT, a target molecular system in propa-
341 gation is automatically and implicitly maintained on its manifold, so the challenge of searching for
342 CVs is met implicitly. Additionally, no bias is necessary and an unnormalized probability density
343 is directly computed for each visited configuration.

344 **Toward computation driven molecular sciences**

345 Recent NNFF has demonstrated significant improvement in accuracy,^{38,58-60} albeit with accompa-
346 nying reduction of efficiency when compared with conventional atomistic MD simulations. With
347 further development of density estimation/fitting, local distributions may be built from near quan-
348 tum accuracy of NNFF based all atom simulations, and subsequently utilized to compose global
349 distributions via dynamic assembly of local distributions as described by the LDT. Such combi-

350 nation may realize long-desired near-quantum accuracy and superior efficiency beyond conven-
351 tional coarse grained models. With corresponding dramatic improvement of efficiency brought by
352 LDT, nanotechnology research may experience a transition from experiment driven to computation
353 driven as spatial and time scales will be accessible by present and computational facility expected
354 in a few years.

355 For computational molecular biology, lack of data is apparent as exemplified by AI based
356 protein structure prediction, design and refinement studies where solvent and thermodynamic con-
357 ditions need to be ignored. Deficiency of structural data is even more severe for denatured states
358 of proteins, nucleic acids and other biomolecular systems (e.g. membranes). Presently, model-
359 ing of diverse thermodynamic and solvent conditions and denatured states relies heavily on all
360 atom MD simulations, which are limited to micro-second time scales in routine investigations of
361 typical proteins for small research groups, and simulation of large complexes and more extensive
362 biomolecular systems is much more challenging. Development of LDT for efficient and accurate
363 construction of local distributions, when combined with one-time near quantum level MD simu-
364 lations for general biomolecular systems has the potential of bridging this gap, and realize rou-
365 tine simulations of large molecular complexes on realistic time scales (mini-seconds and longer).
366 Many present experiment dominated molecular biology research (e.g. protein-protein interactions
367 and protein-drug interactions) may experience transition to computation driven with dramatically
368 improved efficiency. This is especially true for proteins and other biomolecules that are marginally
369 stable and hard to express and store under regular experimental conditions.

370 Establishment of a chain of tools from high level first principle calculations to simulation of
371 large complex molecular systems has been long standing wish for molecular simulation commu-
372 nity. Conventionally, coarse-graining has been the only available option and has made great contri-
373 butions. Development and implementation of LDT in various general molecular systems provides
374 a potential alternative pathway in this regard. However, to realize the potential, significant effort is
375 necessary for development of algorithms in fitting local distributions for a wide variety of molec-
376 ular systems. Condensed matter in general, and biological systems in particular, are organized in

377 hierarchical structures with distinct correlation patterns over different length and time scales. Such
378 characteristics was well summarized by Anderson⁶¹ decades ago and significant efforts have been
379 invested in multi-scale algorithm development in many subjects.⁶²⁻⁶⁵ As discussed above, local dis-
380 tributions are essentially manifolds of local regions under various composition and environmental
381 conditions. The specific meaning of “local” is dependent upon definition of comprising unit on the
382 one hand , and upon length scales on the other hand. Implementation of LDT on multiple scales,
383 and how should it interact with CG or evolve independently, is a fully open field awaits intensive
384 exploration.

385 **Two distinct ways of averaging**

386 Conventional FF parameterization is fundamentally a construction of potential of mean force
387 (PMF)^{66,67} by integration/averaging as shown below:

$$388 \quad U(x) = \int U(x, y) dy \quad (6)$$

389 For fitting of atomistic FF from *ab initio* calculations, y correspond to electronic DOF, for fitting
390 of CG FF from atomistic simulations, y correspond to all atomic DOFs other than CG sites. PMF
391 accurately reproduce behavior of variable x when a time scale separation exists between x and y .
392 Therefore, conventional molecular simulation framework is based on the idea of PMF.

393 Local distributions are clearly results of statistical averaging based on data obtained from ex-
394 pensive local sampling, either through experimental or computational approaches. Essentially,
395 relative frequency of visiting many different configurations are recorded. However, there is no
396 explicit reduction of variables in this process as in the case of PMF integration in FF parameteri-
397 zation (i.e. resolution is maintained). These statements seem to be contradictory as the process of
398 averaging inevitably results in annihilation of some details. One would certainly like to know what
399 is annihilated during the averaging process of fitting local distributions. It is important to note that
400 in computers there is no strictly “continuous” variables anymore as everything is stored by discrete

401 “boxes” in CPU registers, memory chips and hard drives. So all modeling in computer is per-
402 formed on lattices defined by float point number discretization! In fitting of local distributions via
403 neural networks, while input of molecular configurations has the resolution of lattices defined by
404 selected float point digits, there is probably further implicit merging (coarse graining) of different
405 lattice boxes not necessarily uniformly both on different dimensions and on different positions of
406 the same dimension. Such implicit and adaptive annihilation of resolution on various places of the
407 configurational space by the fitting machinery (neural networks) is schematically illustrated in Fig.
408 5. Therefore, LDT opens a distinctive path of averaging based on implicit adaptive configurational
409 space discretization (CSD) instead of explicit integrating out selected DOFs adopted by PMF.

410 Ultimately specifics of such heterogeneous CSD are likely to be determined by details of loss
411 function, network architecture, optimization process and their interactions. However, presently,
412 how such implicit process relates to corresponding neural networks is not transparent. There is
413 no published research on neural networks regarding this topic to the best of my knowledge. Un-
414 derstanding such implicit CSD is likely an essential step to be accomplished in constructing trans-
415 parent white box neural networks. Manual configuration space discretization has been performed
416 to facilitate free energy analysis.⁶⁸ However, proper CSD strategy is usually different for distinct
417 molecular systems and is not necessarily achievable even after significant human efforts. There-
418 fore, to develop explicit, easy-to-manipulate and automatically adaptive schemes for CSD in fitting
419 behavior of neural networks is an important open field to explore.

420 **Conclusions and prospects**

421 RLS in molecular simulations consumes large amount of computational resources on the one hand
422 and slow down exploration of relevant research fields dramatically on the other hand. The LFEL
423 approach was developed to address RLS previously. However, the formulation and its exemplary
424 implementation in protein structural refinement, while demonstrated tremendous potentials, is lim-
425 ited to a single set of given environmental conditions. Here I propose the local distribution theory

426 to generalize LFEL to address variable environmental conditions and near-equilibrium application
427 scenarios. As a matter of fact, essentially all biological systems are off equilibrium to various ex-
428 tent. Despite the simple theoretical proposal presented here, extending implementation of LDT to
429 near-equilibrium poses great challenges and significant exploratory efforts are necessary. Theoret-
430 ical connection and fundamental differences of LDT with metadynamics, RPDD based AI-driven
431 protein structural research, and PMF based framework of conventional molecular simulation in
432 general are discussed. It is hoped that discussions and speculations herein stimulate more interest
433 and attract more scientists in further development and application of the local distribution theory.

434 **Acknowledgement**

435 I thank Professor Jingkai Gu for encouragement and Professor Yaoqi Zhou for comments when
436 this theory was conceived.

437 **References**

- 438 (1) Dror, R. O.; Dirks, R. M.; Grossman, J.; Xu, H.; Shaw, D. E. Biomolecular Simulation: A
439 Computational Microscope for Molecular Biology. *Annual Review of Biophysics* **2012**, *41*,
440 429–452, PMID: 22577825.
- 441 (2) Bedrov, D.; Piquemal, J.-P.; Borodin, O.; MacKerell, A. D., Jr.; Roux, B.; Schroeder, C.
442 Molecular Dynamics Simulations of Ionic Liquids and Electrolytes Using Polarizable Force
443 Fields. *CHEMICAL REVIEWS* **2019**, *119*, 7940–7995.
- 444 (3) Rudzinski, J. F.; Noid, W. G. Coarse-graining entropy, forces, and structures. *Journal of*
445 *Chemical Physics* **2011**, *135*.
- 446 (4) Marrink, S. J.; Tieleman, D. P. Perspective on the martini model. *Chemical Society Reviews*
447 **2013**, *42*, 6801–6822.

- 448 (5) Noid, W. G. Perspective: Coarse-grained models for biomolecular systems. *Journal of Chem-*
449 *ical Physics* **2013**, *139*.
- 450 (6) Saunders, M. G.; Voth, G. A. Coarse-graining methods for computational biology. *Annual*
451 *Review of Biophysics* **2013**, *42*, 73–93.
- 452 (7) Ruff, K. M.; Harmon, T. S.; Pappu, R. V. CAMELOT: A machine learning approach for
453 Coarse-grained simulations of aggregation of block-copolymeric protein sequences. *Journal*
454 *of Chemical Physics* **2015**, *143*, 1–19.
- 455 (8) Kmiecik, S.; Gront, D.; Kolinski, M.; Wieteska, L.; Dawid, A. E.; Kolinski, A. Coarse-
456 Grained Protein Models and Their Applications. *Chemical Reviews* **2016**, *116*, 7898–7936.
- 457 (9) Hafner, A. E.; Krausser, J.; Saric, A. Minimal coarse-grained models for molecular self-
458 organisation in biology. *CURRENT OPINION IN STRUCTURAL BIOLOGY* **2019**, *58*, 43–
459 52.
- 460 (10) Sambasivan, R.; Das, S.; Sahu, S. K. A Bayesian perspective of statistical machine learning
461 for big data. *COMPUTATIONAL STATISTICS* **2020**, *35*, 893–930.
- 462 (11) Joshi, S. Y.; Deshmukh, S. A. A review of advancements in coarse-grained molecular dynam-
463 ics simulations. *Molecular Simulation* **2020**, *0*, 1–18.
- 464 (12) Gkeka, P. et al. Machine Learning Force Fields and Coarse-Grained Variables in Molecular
465 Dynamics: Application to Materials and Biological Systems. *Journal of Chemical Theory*
466 *and Computation* **2020**, *16*, 4757–4775, PMID: 32559068.
- 467 (13) Bernardi, R. C.; Melo, M. C. R.; Schulten, K. Enhanced sampling techniques in molecular dy-
468 namics simulations of biological systems. *BIOCHIMICA ET BIOPHYSICA ACTA-GENERAL*
469 *SUBJECTS* **2015**, *1850*, 872–877.
- 470 (14) Mlynsky, V.; Bussi, G. Exploring RNA structure and dynamics through enhanced sampling
471 simulations. *CURRENT OPINION IN STRUCTURAL BIOLOGY* **2018**, *49*, 63–71.

- 472 (15) Yang, Y. I.; Shao, Q.; Zhang, J.; Yang, L.; Gao, Y. Q. Enhanced sampling in molecular
473 dynamics. *Journal of Chemical Physics* **2019**, *151*.
- 474 (16) Wang, A.-h.; Zhang, Z.-c.; Li, G.-h. Advances in Enhanced Sampling Molecular Dynamics
475 Simulations for Biomolecules. *CHINESE JOURNAL OF CHEMICAL PHYSICS* **2019**, *32*,
476 277–286.
- 477 (17) Cao, X.; Tian, P. Molecular free energy optimization on a computational graph. *RSC Adv.*
478 **2021**, *11*, 12929–12937.
- 479 (18) Cao, X.; Tian, P. “Dividing and Conquering” and “Caching” in Molecular Modeling. *Inter-*
480 *national Journal of Molecular Sciences* **2021**, *22*.
- 481 (19) Long, S.; Tian, P. A simple neural network implementation of generalized solvation free
482 energy for assessment of protein structural models. *RSC Advances* **2019**, *9*, 36227–36233.
- 483 (20) Senior, A. W. et al. Improved protein structure prediction using potentials from deep learning.
484 *Nature* **2020**, *577*, 706–710.
- 485 (21) Suh, D.; Lee, J. W.; Choi, S.; Lee, Y. Recent Applications of Deep Learning Methods on
486 Evolution- and Contact-Based Protein Structure Prediction. *International Journal of Molec-*
487 *ular Sciences* **2021**, *22*.
- 488 (22) Pakhrin, S. C.; Shrestha, B.; Adhikari, B.; KC, D. B. Deep Learning-Based Advances in
489 Protein Structure Prediction. *International Journal of Molecular Sciences* **2021**, *22*.
- 490 (23) Skolnick, J.; Gao, M. The role of local versus nonlocal physicochemical restraints in deter-
491 mining protein native structure. *Current Opinion in Structural Biology* **2021**, *68*, 1–8, Protein-
492 Carbohydrate Complexes and Glycosylation Sequences and Topology.
- 493 (24) Ju, F.; Zhu, J.; Shao, B.; Kong, L.; Liu, T.-Y.; Zheng, W.-M.; Bu, D. CopulaNet: Learning
494 residue co-evolution directly from multiple sequence alignment for protein structure predic-
495 tion. *Nature Communications* **2021**, *12*, 2535.

- 496 (25) Jing, X.; Xu, J. Improved protein model quality assessment by integrating sequential and
497 pairwise features using deep learning. *Bioinformatics* **2020**, *36*, 5361–5367.
- 498 (26) Zhao, K.-l.; Liu, J.; Zhou, X.-g.; Su, J.-z.; Zhang, G.-j. Structural bioinformatics MMpred : a
499 distance-assisted multimodal conformation sampling for de novo protein structure prediction.
500 *Bioinformatics* **2021**, 1–8.
- 501 (27) Xia, Y.-h.; Peng, C.-x.; Zhou, X.-g.; Zhang, G.-j. Structural bioinformatics A Sequential
502 Niche Multimodal Conformational Sampling Algorithm for Protein Structure Prediction.
503 *Bioinformatics* **2021**, 1–9.
- 504 (28) Wu, F.; Xu, J. Deep template-based protein structure prediction. *PLoS computational biology*
505 **2021**, *17*, 1–18.
- 506 (29) Zhang, H.; Bei, Z.; Xi, W.; Hao, M.; Ju, Z. Evaluation of residue-residue contact prediction
507 methods : From retrospective to prospective. *PLOS Comput. Biol.* **2021**, *17*, 1–33.
- 508 (30) Mackerell Jr., A. D. Empirical force fields for biological macromolecules: Overview and
509 issues. *Journal of Computational Chemistry* **2004**, *25*, 1584–1604.
- 510 (31) Kumar, A.; Yoluk, O.; MacKerell Jr., A. D. FFParam: Standalone package for CHARMM
511 additive and Drude polarizable force field parametrization of small molecules. *Journal of*
512 *Computational Chemistry* **2020**, *41*, 958–970.
- 513 (32) Oweida, T. J.; Kim, H. S.; Donald, J. M.; Singh, A.; Yingling, Y. G. Assessment of AMBER
514 Force Fields for Simulations of ssDNA. *Journal of Chemical Theory and Computation* **2021**,
515 *17*, 1208–1217, PMID: 33434436.
- 516 (33) Huai, Z.; Shen, Z.; Sun, Z. Binding Thermodynamics and Interaction Patterns of Inhibitor-
517 Major Urinary Protein-I Binding from Extensive Free-Energy Calculations: Benchmarking
518 AMBER Force Fields. *Journal of Chemical Information and Modeling* **2021**, *61*, 284–297,
519 PMID: 33307679.

- 520 (34) Alford, R. F. et al. The Rosetta All-Atom Energy Function for Macromolecular Modeling
521 and Design. *Journal of Chemical Theory and Computation* **2017**, *13*, 3031–3048, PMID:
522 28430426.
- 523 (35) Sasse, A.; de Vries, S. J.; Schindler, C. E. M.; de Beauchêne, I. C.; Zacharias, M. Rapid
524 Design of Knowledge-Based Scoring Potentials for Enrichment of Near-Native Geometries
525 in Protein-Protein Docking. *PLOS ONE* **2017**, *12*, 1–19.
- 526 (36) Narykov, O.; Bogatov, D.; Korkin, D. DISPOT: a simple knowledge-based protein domain
527 interaction statistical potential. *Bioinformatics* **2019**, *35*, 5374–5378.
- 528 (37) Noé, F.; Tkatchenko, A.; Müller, K.-R.; Clementi, C. Machine Learning for Molecular Sim-
529 ulation. *Annual Review of Physical Chemistry* **2020**, *71*, 361–390, PMID: 32092281.
- 530 (38) Gkeka, P. et al. Machine Learning Force Fields and Coarse-Grained Variables in Molecular
531 Dynamics: Application to Materials and Biological Systems. *Journal of Chemical Theory
532 and Computation* **2020**, *16*, 4757–4775, PMID: 32559068.
- 533 (39) Dowsland, K. A.; Thompson, J. M. In *Handbook of Natural Computing*; Rozenberg, G.,
534 Bäck, T., Kok, J. N., Eds.; Springer Berlin Heidelberg: Berlin, Heidelberg, 2012; pp 1623–
535 1655.
- 536 (40) Behler, J. Perspective: Machine learning potentials for atomistic simulations. *Journal of
537 Chemical Physics* **2016**, *145*.
- 538 (41) Parzen, E. On Estimation of a Probability Density Function and Mode. *The Annals of Math-
539 ematical Statistics* **1962**, *33*, 1065 – 1076.
- 540 (42) Uria, B.; Côté, M.-A.; Gregor, K.; Murray, I.; Larochelle, H. Neural Autoregressive Distribu-
541 tion Estimation. *Journal of Machine Learning Research* **2016**, *17*, 1–37.
- 542 (43) Kobyzev, I.; Brubaker, M. A. Normalizing Flows: Introduction and Ideas. *ArXiv* **2019**, 1–35.

- 543 (44) Papamakarios, G.; Nalisnick, E. Normalizing Flows for Probabilistic Modeling and Infer-
544 ence. *ArXiv* **2019**, 1–60.
- 545 (45) Noé, F.; Olsson, S.; Kohler, J.; Wu, H. Boltzmann generators: Sampling equilibrium states of
546 many-body systems with deep learning. *Science* **2019**, *365*, eaaw1147.
- 547 (46) Liu, Q.; Xu, J.; Jiang, R.; Hung, W. Density estimation using deep generative neural net-
548 works. *Proceedings of the National Academy of Sciences* **2021**, *118*.
- 549 (47) Cun, Y.; Huang, F. Loss functions for discriminative training of energy-based models. AIS-
550 TATS 2005 - Proceedings of the 10th International Workshop on Artificial Intelligence and
551 Statistics. 2005; pp 206–213, 10th International Workshop on Artificial Intelligence and
552 Statistics, AISTATS 2005 ; Conference date: 06-01-2005 Through 08-01-2005.
- 553 (48) BakIr, G.; Hofmann, T.; Schölkopf, B.; Smola, A. J.; Taskar, B.; Vishwanathan, S. *Predicting*
554 *Structured Data*; The MIT Press, 2007.
- 555 (49) Zhao, J.; Mathieu, M.; Lecun, Y.; Artificial, F. Energy-based generative adversarial networks.
556 *ArXiv* **2017**, 1–17.
- 557 (50) Liu, M.; Yan, K.; Oztekin, B.; Ji, S. GraphEBM: Molecular Graph Generation with Energy-
558 Based Models. *ArXiv* **2020**,
- 559 (51) Mordatch, I. Compositional Visual Generation with Energy Based Models. *ArXiv* **2020**,
- 560 (52) Grathwohl, W.; Duvenaud, D. Your classifier is secretly an energy based model and you
561 should treat it like one. *ArXiv* **2020**, 1–23.
- 562 (53) Chan, K. H. R.; Yu, Y.; You, C.; Qi, H.; Wright, J.; Ma, Y. ReduNet: A White-box Deep
563 Network from the Principle of Maximizing Rate Reduction. 2021.
- 564 (54) Jing, X.; Xu, J. Fast and effective protein model refinement using deep graph neural networks.
565 *Nature Computational Science* **2021**, *1*, 462–469.

- 566 (55) Jumper, J. et al. Highly accurate protein structure prediction with AlphaFold. *Nature* **2021**,
- 567 (56) Baek, M. et al. Accurate prediction of protein structures and interactions using a three-track
568 neural network. *Science* **2021**, 373, abj8754.
- 569 (57) Frenkel, D.; Smit, B. In *Understanding Molecular Simulation (Second Edition)*, second edi-
570 tion ed.; Frenkel, D., Smit, B., Eds.; Academic Press: San Diego, 2002; pp 139–163.
- 571 (58) Zhang, L.; Han, J.; Wang, H.; Car, R.; E, W. Deep Potential Molecular Dynamics: A Scalable
572 Model with the Accuracy of Quantum Mechanics. *Phys. Rev. Lett.* **2018**, 120, 143001.
- 573 (59) Bedolla, E.; Padierna, L. C.; Castañeda-Priego, R. Machine learning for condensed matter
574 physics. *Journal of Physics: Condensed Matter* **2020**, 33, 053001.
- 575 (60) Lu, D.; Wang, H.; Chen, M.; Lin, L.; Car, R.; E, W.; Jia, W.; Zhang, L. 86 PFLOPS Deep
576 Potential Molecular Dynamics simulation of 100 million atoms with ab initio accuracy. *Com-
577 puter Physics Communications* **2021**, 259, 107624.
- 578 (61) Anderson, P. More is different. *Science* **1972**, 177, 393–396.
- 579 (62) Franco, A. A.; Rucci, A.; Brandell, D.; Frayret, C.; Gaberscek, M.; Jankowski, P.; Johans-
580 son, P. Boosting Rechargeable Batteries R&D by Multiscale Modeling: Myth or Reality?
581 *Chemical Reviews* **2019**, 119, 4569–4627, PMID: 30859816.
- 582 (63) Henning, P.; Peterseim, D. Oversampling for the Multiscale Finite Element Method. *Multi-
583 scale Modeling & Simulation* **2013**, 11, 1149–1175.
- 584 (64) Abdulle, A.; Weinan, E.; Engquist, B.; Vanden-Eijnden, E. The heterogeneous multiscale
585 method. *Acta Numerica* **2012**, 21, 1?87.
- 586 (65) Ramstead, M. J. D.; Kirchhoff, M. D.; Constant, A.; Friston, K. J. Multiscale integration:
587 beyond internalism and externalism. *Synthese* **2021**, 198, 41–70.

- 588 (66) Kirkwood, J. G. Statistical Mechanics of Fluid Mixtures. *Journal of Chemical Physics* **1935**,
589 3, 300–313.
- 590 (67) Roux, B. The calculation of the potential of mean force using computer simulations. *Com-*
591 *puter Physics Communications* **1995**, 91, 275–282.
- 592 (68) Wang, K.; Long, S.; Tian, P. Configurational space discretization and free energy calculation
593 in complex molecular systems. *Scientific Reports* **2016**, 6, 22217.

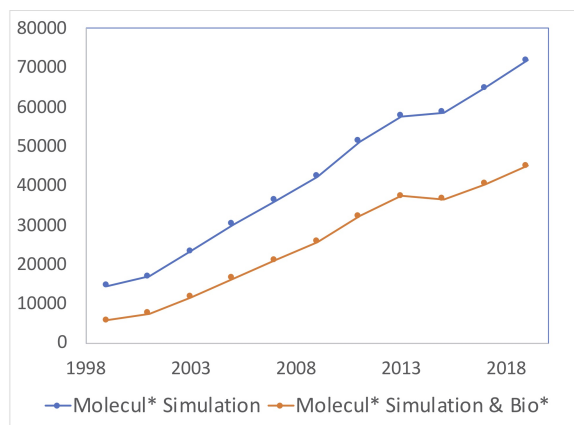


Figure 1: The number of publications retrieved from web of science on Jun. 1st 2021 with subject word "molecul* simulation" and "molecul* simulation & bio" respectively. The corresponding time frame is every two years starting from 1999. The first data point is the number of papers published in year 1999 and 2000.

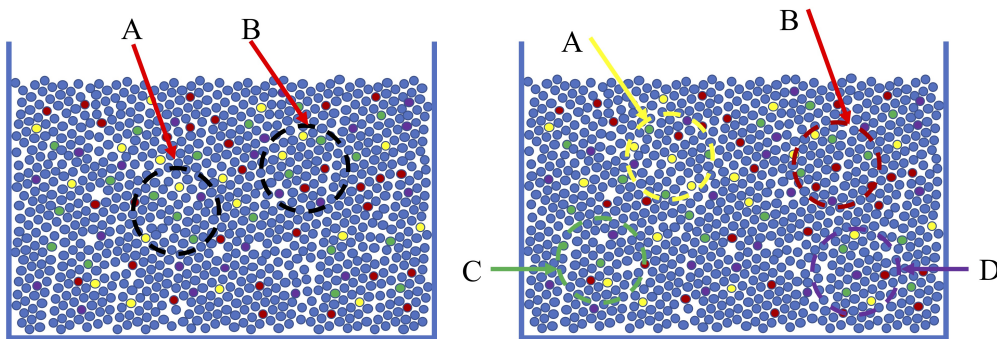


Figure 2: Schematic illustration of RLS. Left: the spatial perspective. A) and B) are two different spherical bulk spaces. We expect the same local distributions after sufficiently long simulations of the whole molecular system. In such cases, spherical and partial spherical spaces near or on interfaces have different local distributions from that of the bulk, special treatment of such spherical spaces engenders significant difficulty. Right: indistinguishable particle and GSFE perspective. All particles of the same species are indistinguishable, so should be local distributions of local regions defined by spherical spaces with such a particle as the origin. This removes the need for special treatment of all interfacial issues as different interfaces may be simply defined as more cases of particle packing surrounding a given particle with well defined statistical weight under given thermodynamic and environmental conditions. A), B), C) and D) are examples of surrounding local regions of different particle species.

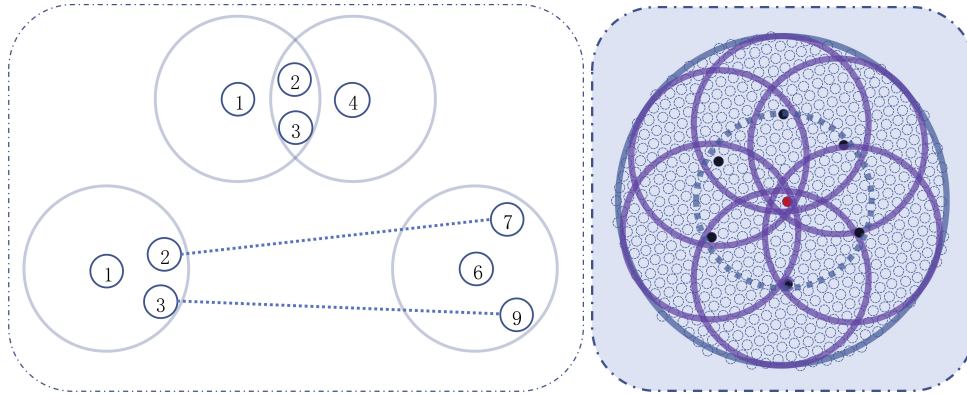


Figure 3: Schematic representation of the short range, mediated interactions and long range interactions as implemented in ref. Left: particles (1,2,3), (2,3,4) and (6,7,9) are directly interacting with short range interactions. (1,4) are interacting through mediation by (2,3), (2,7) and (3,9) have direct long range interactions. Right: here the focus is the central red particle, which define a region with boundary being shown as dotted partially transparent blue line. Each of all other particles within this region defines a local distribution, six of the most further of such regions are represented as purple circles. The central red particle experience forces from all of local distributions surrounding each of its neighbors. In this way, short range and mediated interactions are effectively accounted for simultaneously. In summary, for the central red particle, it experiences short range interactions from particles within the dotted partial transparent blue circle, mediated interactions from particles between the dotted blue circle and large solid blue circle, long range interactions from the region outside the large blue circle.

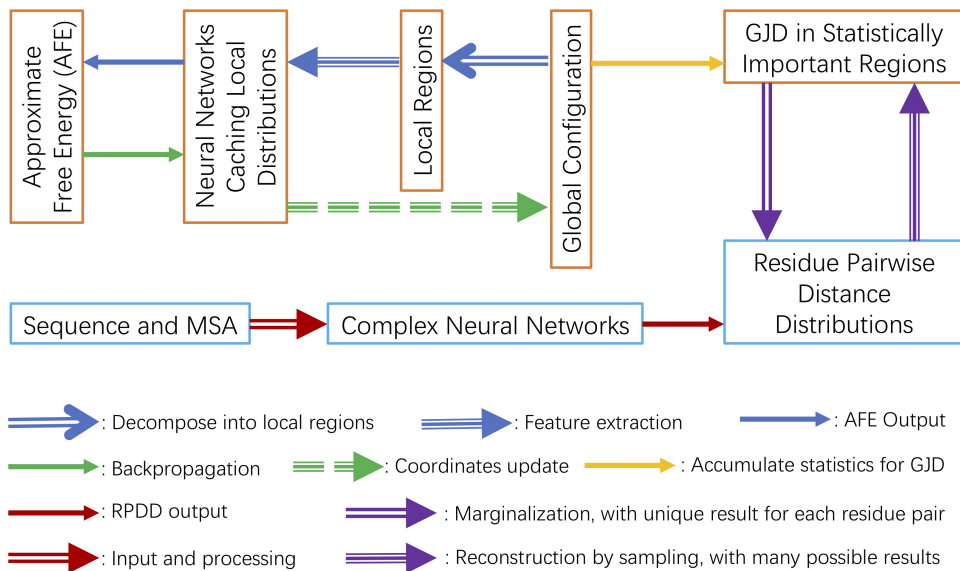


Figure 4: Schematic comparison between LDT based end-to-end protein structure modeling (top orange boxes) and mainstream RPDD based protein structure prediction and refinement schemes (bottom blue boxes). It is important to note that LDT based modeling aims to generate the GJD, which is the most comprehensive information for any complex molecular system and is generally applicable. The marginalization from the GJD to pairwise residue distance distributions is an irreversible process with deterministic results and significant information loss on correlations among different pairwise distances. The converse process is a highly expensive process with sampling and optimization involved, due to complexity of correlations among different distances, resulting global distribution is highly dependent both on initialization and the optimization procedures.

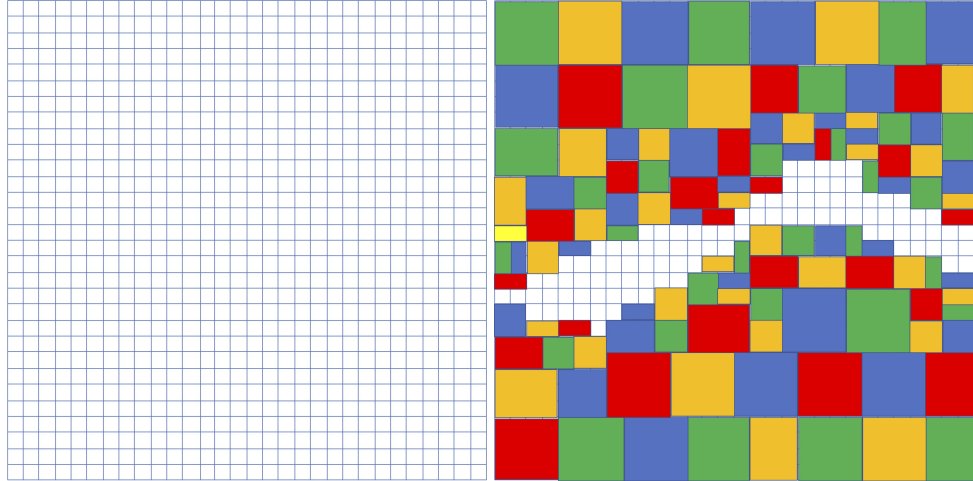


Figure 5: Schematic illustration of CSD. Left: natural discretization of two dimensional configurational space by float point digits. Right: a imagined heterogeneous CSD resulted from fitting of neural network on local distributions, and the highest density is supposedly in the white region where CSD is as fine as lattices determined by float point digits. Qualitatively, finer discretization corresponds to region with high data density and coarser discretization corresponds to region with lower data density.